

This article was downloaded by:

On: 25 January 2011

Access details: *Access Details: Free Access*

Publisher *Taylor & Francis*

Informa Ltd Registered in England and Wales Registered Number: 1072954 Registered office: Mortimer House, 37-41 Mortimer Street, London W1T 3JH, UK



Separation Science and Technology

Publication details, including instructions for authors and subscription information:

<http://www.informaworld.com/smpp/title~content=t713708471>

Preconcentration and Determination of Metal Ions in Commercial Ethanol Used as Fuel for Automotive Engines

Newton Luiz Dias Filho^a; Reginaldo Mendonça Costa^a; Giovana Lopes Okajima^a

^a Departamento de Física e Química, Unesp-Universidade Estadual Paulista, Ilha Solteira, SP, Brazil

To cite this Article Filho, Newton Luiz Dias , Costa, Reginaldo Mendonça and Okajima, Giovana Lopes(2008) 'Preconcentration and Determination of Metal Ions in Commercial Ethanol Used as Fuel for Automotive Engines', Separation Science and Technology, 43: 3, 624 — 641

To link to this Article: DOI: 10.1080/01496390701787065

URL: <http://dx.doi.org/10.1080/01496390701787065>

PLEASE SCROLL DOWN FOR ARTICLE

Full terms and conditions of use: <http://www.informaworld.com/terms-and-conditions-of-access.pdf>

This article may be used for research, teaching and private study purposes. Any substantial or systematic reproduction, re-distribution, re-selling, loan or sub-licensing, systematic supply or distribution in any form to anyone is expressly forbidden.

The publisher does not give any warranty express or implied or make any representation that the contents will be complete or accurate or up to date. The accuracy of any instructions, formulae and drug doses should be independently verified with primary sources. The publisher shall not be liable for any loss, actions, claims, proceedings, demand or costs or damages whatsoever or howsoever caused arising directly or indirectly in connection with or arising out of the use of this material.

Preconcentration and Determination of Metal Ions in Commercial Ethanol Used as Fuel for Automotive Engines

Newton Luiz Dias Filho, Reginaldo Mendonça Costa,
and Giovana Lopes Okajima

Departamento de Física e Química, Unesp-Universidade Estadual Paulista, Ilha Solteira, SP, Brazil

Abstract: The present investigation reports the synthesis, characterization, and adsorption properties of a new nanomaterial based on organomodified silsesquioxane nanocages. The adsorption isotherms for CuCl_2 , CoCl_2 , ZnCl_2 , NiCl_2 , and FeCl_3 from ethanol solutions were performed by using the batchwise method. The equilibrium condition is reached very quickly (3 min), indicating that the adsorption sites are well exposed. The results obtained in the flow experiments, showed a recovery of *ca.* 100% of the metal ions adsorbed in a column packed with 2 g of the nanomaterial, using 5 mL of 1.0 mol L^{-1} HCl solution as eluent. The sorption-desorption of the metal ions made possible the development of a method for preconcentration and determination of metal ions at trace level in commercial ethanol, used as fuel for car engines. The values determined by recommended method for plants 1, 2, and 3 indicated an amount of copper of 51, 60, and 78 $\mu\text{g L}^{-1}$, and of iron of 2, 15, and 13 $\mu\text{g L}^{-1}$, respectively. These values are very close to those determined by conventional analytical methods. Thus, these similar values demonstrated the accuracy of the determination by recommended method.

Keywords: Fuel ethanol, preconcentration, adsorption, isotherms of adsorption, transition-metal ions

Received 30 April 2007, Accepted 30 September 2007

Address correspondence to Newton Luiz Dias Filho, Departamento de Física e Química, Unesp-Universidade Estadual Paulista, Av. Brasil, 56-Centro, Caixa Postal 31, 15385-000, Ilha Solteira, SP, Brazil. Fax: (0055) (18) 3742-4868; E-mail: nldias@dfq.feis.unesp.br

INTRODUCTION

Polyhedral oligomeric silsesquioxanes (POSS) have been the subject of considerable theoretical and practical interest (1–4). POSS, with the general formula $(RSiO_{1.5})_n$, possess cubic silica cores with 0.53 nm diameter and a spherical radius of 1–3 nm including peripheral organic units. Reviews on this field were published by Baney et al., Li et al., and Calzaferri (5–7). Through their eight Si vertices, these nanoplatforms may be covalently linked to a plethora of organic groups which may offer attractive properties and applications, such as ligands for transition-metal ions (8–12).

On the other hand, the organofunctionalized silicas have been the subject of considerable interest due to its multiple uses in high-efficiency liquid chromatography, in preconcentration and separation processes, as an ion exchanger and as a chemical sensor (13–20).

Other materials, such as epoxy resin, biopolymer, chitosan beads, magnetite nanoparticles coated with nonylthiourea, have also been used in preconcentration and separation processes (21–24).

In Brazil, commercial ethanol designates a mixture of ethanol with a low percentage of water. It can be used in diverse fields such as in alcohol chemistry or as automotive engine fuels.

The development of methods to determine traces of metals has been one aspect of interest in the research on ethanol as a fuel (16, 19, 20, 25, 26).

However, the application of organomodified silsesquioxane nanocages for cation removal from commercial ethanol, used as fuel for car engines, have not yet been explored.

These metals result from the alcohol extraction operation from sugar cane. The presence of some metal ions in ethanol fuel can induce corrosion in the vehicle components in contact with the liquid (16, 25, 26). The metals normally found in commercial ethanol are Cu(II), Fe(III), Zn(II), and Ni(II).

The direct determination of trace metals in fuel ethanol by conventional analytical methods can be performed after a time-consuming liquid evaporation procedure prior to any measurements (16). In particular, a column packed with an adsorbent material in line with a flow analysis system can considerably improve the method of analysis extending the limit of detection to lower concentrations.

The determination of metal ions in fuel ethanol after preconcentration on organomodified silica and barium phosphate have been reported (16, 25, 26). However, materials prepared this way in most of the cases presented a low degree of organofunctionalization and/or a wide time interval for reaching the equilibrium condition in the adsorption process.

The objective of this research was the preparation of the octakis[3-(3-amino-1,2,4-triazole)propyl]octasilsesquioxane in order to find a new nano-material potentially useful for analytical purposes, such as for separation and determination of the metal ions present in commercial ethanol, used as

fuel for car engines. It is expected that this nanomaterial presents some additional advantages for adsorption of these metal ions, such as a high degree of organofunctionalization, large adsorption capacity, great stability, reutilization possibility, rapidity in reaching the equilibrium and high mechanical resistance.

EXPERIMENTAL

Chemicals and Reagents

3-Chloropropyltriethoxysilane, 3-amino-1,2,4-triazole, hydrochloric acid, methanol were purchased from Aldrich Chemical Company and used as received. Dimethylformamide, hexane and methanol was purchased from Lancaster Synthesis Company and used without further purification.

Preparations

Synthesis of the Precursor Octakis(3-Chloropropyl)Octasilsesquioxane

3-Chloropropyltriethoxysilane (225 mL) was added to a stirred mixture of methanol (4 L) and concentrated hydrochloric acid (35 mL) under a slow continuous nitrogen purge. The reaction mixture was allowed to stir for 6 weeks. The resultant solution was then filtered and dried to give a white solid (37% yield). Elemental analysis: anal.: calcd.: C 27.78%, H 4.74%, Cl. 27.40%; found: C 27.68%, H 4.74%, Cl. 27.30%. GPC: Mn = 950, Mw = 1027, PDI = 1.08, calcd: Mw = 1037 g/mol. $^{13}\text{CNMR}$ (δ , ppm): 10.56 (CH_2Si), 27.55 (CCH_2C), 49.56 (ClCH_2). ^{29}Si RMN (δ , ppm): -68.00 (OSiCH_2) · FTIR (KBr, cm^{-1}): 3650–3200 (ν O-H), 2950 (ν C-H), 1250 (ν Si-C), \sim 1110–1030, 770 (ν Si-O-Si).

Synthesis of the Nanomaterial Octakis[3-(3-amino-1,2,4-triazole)propyl] Octasilsesquioxane (ATZ-SSQ)

To a stirred solution of octakis(3-chloropropyl)octasilsesquioxane (21.36 g, 0.020 mol) in anhydrous dimethylformamide (60 mL) was added 3-amino-1,2,4-triazole (19.30 g, 0.229 mol). The mixture was allowed to reflux over a period of 12 h. The resulting octakis[3-(3-amino-1,2,4-triazole)propyl]octasilsesquioxane (ATZ-SSQ), a pale yellow solid, was filtered, washed with dimethylformamide, ethanol and methanol, and dried in vacuo (80% yield). Elemental analysis: calcd.: 33.88%, 5.13%, 31.61%; found: C 33.78%, H 5.09%, N 31.55%. GPC: Mn = 1297, Mw = 1400, PDI = 1.08, calcd: Mw = 1417 g/mol. $^{13}\text{CNMR}$ (δ , ppm): 8.13 (CH_2Si), 24.00 (CCH_2C), 49.90 (NCH_2), 149.60 (NCHN), 158.00 ($\text{NC}(\text{NH}_2)\text{N}$). ^{29}Si RMN (δ , ppm):

–68,50 (OSiCH₂). FTIR (KBr, cm^{−1}): 3650–3200 (ν O-H); 2950 (ν C-H), 1689 (νC=N), 1620 (δN-H), 1320, 1450 (ν C-N), 1250 (ν Si-C); ~1110–1030, 770 (ν Si-O-Si).

Spectroscopy

¹³CNMR and ²⁹Si-NMR spectra were recorded on a BRUKER DRX 400 spectrometer and obtained at 100.6 MHz and 79.48 MHz, respectively.

Gel Permeation Chromatography (GPC). GPC data were measured using a Waters GPC system, equipped with RI and UV detectors, a Styragel column set, and a data capture unite. The system was calibrated using polystyrene standards, with THF used as the eluent.

Fourier transform infrared spectroscopy (FTIR). FTIR spectra were recorded on a Nicolet 670 FT-IR spectrometer (Nicolet Instruments, Madison, WI). About 600 mg of KBr were ground in a mortar and pestle, and a sufficient quantity of the solid sample was ground with KBr to produce a 1wt% mixture resulting in pellets. A minimum of 32 scans was collected at a resolution of 4 cm^{−1}.

Scanning electronic microscopy (SEM). The SEM images of the materials were obtained using JEOL JSM T-300 microscope. The samples were adhered over aluminum holders and covered with a thin layer (20–30 nm) of gold in Sputter Coater Bal-Tec SCD-050.

The X-ray powder diffraction patterns (XRD) were obtained by using a Siemens D 5000 diffractometer with CuK α radiation, submitted to 40 KV, 30 mA, 0.05° s^{−1} and exposed to radiation from 4 up to 40° (2θ).

Isotherms of Adsorption

The isotherms of adsorption for CuCl₂, CoCl₂, ZnCl₂, NiCl₂, and FeCl₃ from ethanol solutions on the ATZ-SSQ were determined by using the batchwise technique. For each isotherm a series of samples containing 0.1 g of the adsorbent in 50.0 mL of ethanol solution with variable concentrations of each metal halide (concentrations between 2 × 10^{−4} and 8 × 10^{−3} mol L^{−1}) was mechanically shaken for 5min at a constant temperature of 298 ± 1 K. The concentration of the metal ion in solution, in equilibrium with solid phase, was determined by atomic adsorption spectrometry. The quantity of adsorbed metal, N_f, in each flask was determined by the equation N_f = (N_a − N_s)/m, where m is the mass of the adsorbent and N_a and N_s are the initial and the equilibrium amount of the number of moles of the metal in the solution phase, respectively. The same adsorption procedure with the untreated silsesquioxane showed that no cation was adsorbed.

Preconcentration and Recovery of the Metal Ions

This study was carried out using a 15 cm length and 0.6 cm inner diameter glass column packed with 2 g of organomodified silsesquioxane. ATZ-SSQ was ground gently using an agate mortar and pestle. ATZ-SSQ consisted of aggregated 0.7-1 μm particles. The particle-size was derived from the sedimentation velocity in the gravitational field. Before placing 2 g of ATZ-SSQ into the column, a small amount of glass wool was placed in the lower part of the column and after placing the sorbent another layer of glass wool was placed in the upper part of the column to prevent loss of the ATZ-SSQ nanomaterial. Initially, the column was washed with ethanol and then 100 mL of 0.50 mg L^{-1} MCl_x ($\text{M} = \text{Co(II)}, \text{Cu(II)}, \text{Ni(II)}, \text{Zn(II)}, \text{and Fe(III)}$) ethanol solutions were percolated through the column with a flow rate of 3.0 mL min^{-1} . The column was washed with 50 mL of ethanol and then the metal was eluted with 5 mL 1.0 mol L^{-1} HCl solution. All fractions obtained during the elution stage were gathered separately and analysed by Flame AAS.

Determination of Metal Ions in Ethanol Fuel

About 250 mL of commercial ethanol samples, used as fuel for car engines, were percolated through the column packed with 2 g of ATZ-SSQ. The adsorbed metal ions were eluted with 5 mL of 1.0 mol L^{-1} HCl solution and the metal ions analysed by Flame AAS.

Determination by AAS

The concentrations of metal ions gathered from the ATZ-SSQ column were determined by Flame AAS according to the standard guidelines of the manufacturers (Spectrometer: Perkin Elmer Analyst 700), choosing resonance lines for the metals and deuterium-arc lamp background correction. For the calibration, synthetic standard solutions containing on 1.0 mol L^{-1} HCl comparable to the samples, were used.

RESULTS AND DISCUSSION

Synthetic Aspects of the ATZ-SSQ Nanomaterial

The synthesis of the ATZ-SSQ was accomplished by a two step process. The synthesis route is outlined in Figs 1 and 2.

The octakis(3-chloropropyl)octasilsesquioxane precursor was prepared in high yield (37% by weight) by HCl catalytic hydrolysis and condensation of

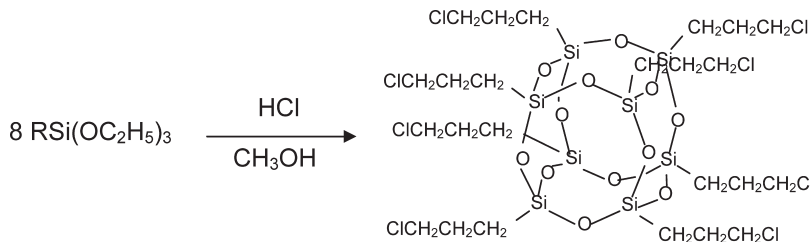


Figure 1. Synthesis of the octakis(3-chloropropyl)octasilsesquioxane.

3-chloropropyltriethoxysilane in methanol at room temperature, as outlined in Fig. 1. The synthesized product was characterized by elemental analysis, GPC, FTIR, ^{13}C and ^{29}Si NMR spectroscopy (see Exp. Sect.).

Octakis(3-chloropropyl)octasilsesquioxane is an excellent precursor, as the $(\text{CH}_2)_3\text{Cl}$ functionalities can be modified to incorporate a host of organic functional groups suitable for various applications. The highly reactive C-Cl groups are readily transformed into other functionalized organic substituents making this silsesquioxane a key starting reagent in building molecular composites.

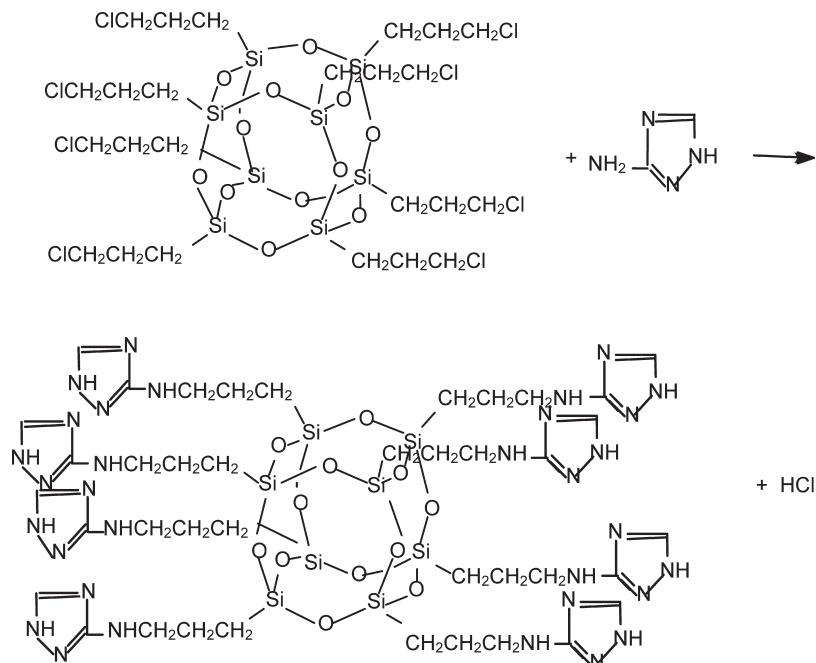


Figure 2. Synthesis of the octakis[3-(3-amino-1,2,4-triazole)propyl]octa silsesquioxane.

The nanocage silsesquioxane cores were covalently linked to 3-amino-1,2,4-triazole molecules through of the eight pendant $(CH_2)_3Cl$ molecular “arms” of the octakis(3-chloropropyl)octasilsesquioxane, resulting in the formulation in which eight [3-(3-amino-1,2,4-triazole)propyl] groups are covalently linked to eight vertices of the silsesquioxane nanoplatforms, forming the octakis[3-(3-amino-1,2,4-triazole)propyl] octasilsesquioxane (ATZ-SSQ) (Fig. 2).

The structure of the ATZ-SSQ was confirmed by elemental analysis, SEM, XRD, GPC, ^{13}C NMR, ^{29}Si NMR, and FTIR (see Exp. Sect.).

Based on the nitrogen elemental analysis (see Exp. Sect.) the density of the organofunctionalization (N_o) was calculated giving a value of 5.63 mmol of 3-amino-1,2,4-triazole molecules per gram of material, confirming that eight 3-amino-1,2,4-triazole molecules are linked to silsesquioxane core. The molecular weight of the ATZ-SSQ determined by GPC ($M_w = 1400$, calcd: $M_w = 1417$ g/mol) confirmed the structure proposed for the ATZ-SSQ, as is shown in Fig. 3.

Scanning electronic microscopy (SEM) measurements of the materials showed that the nonmodified silsesquioxane, namely octakis(hydridosilsesquioxane) $(HSiO_{3/2})_8$, is formed by aggregates of cubic particles (see Figures 4A and 4B). After reaction with [3-(3-amino-1,2,4-triazole)propyl] groups, a new SEM image exhibited the disappearance of the majority of pores (Fig. 4C).

The XRD spectra of nonmodified silsesquioxane and ATZ-SSQ are illustrated in Fig. 5. The X-ray diffraction (XRD) spectrum for the nonmodified silsesquioxane, $(HSiO_{3/2})_8$, is illustrated in Fig. 5A, with the following characteristics 2θ at 7.9, 8.4, 11.04, 18.9, 24.13°. The change of phase and

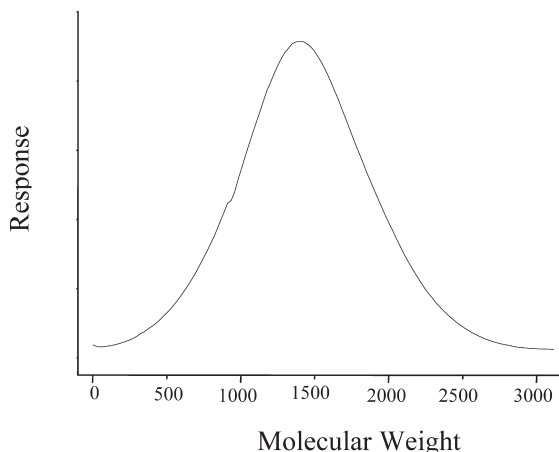


Figure 3. Gel permeation chromatogram of the octakis[3-(3-amino-1,2,4-triazole)-propyl] octasilsesquioxane.

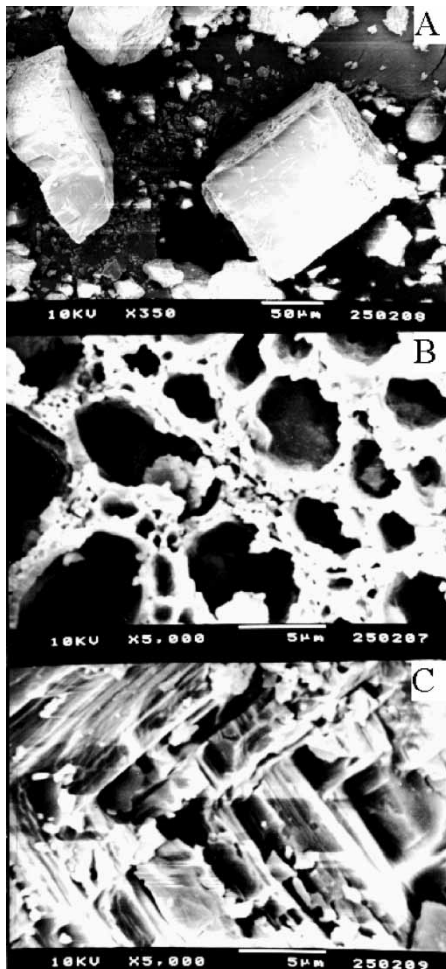


Figure 4. Scanning electron micrograph of: (A) (octakis-hydridosilsesquioxane, $(HSiO_{3/2})_8$, $\times 350$); (B) (octakis-hydridosilsesquioxane, $(HSiO_{3/2})_8$, $\times 5000$); (C) (octakis[3-(3-amino-1,2,4-triazole)propyl] octasilsesquioxane, $\times 5000$).

cristalinity loss of ATZ-SSQ is clear (Fig. 5B). In concordance with Lichtenhan (27), a redistribution of the silicon environment is accompanied by remarkable increases in the line widths as well as shifts in their maximum values.

Figure 6 shows the five resonance peaks that appeared from five different carbon environments associated with the ATZ-SSQ in the ^{13}C NMR (8.13 ($CH_2\text{Si}$), 24.00 ($CCH_2\text{C}$), 49.90 (NCH_2), 149.60 ($NCHN$), and 158.00 ppm ($NC(NH_2)\text{N}$)). The only resonance at -68.50 ppm shown in the ^{29}Si RMN spectrum, in Fig. 7, is assigned to the Q-type silicon

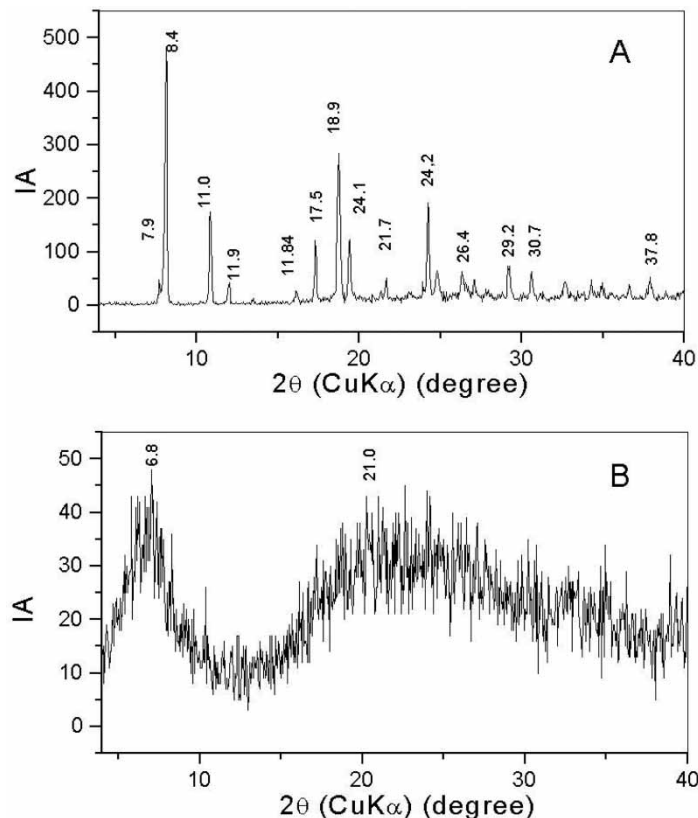


Figure 5. X-ray powder diffraction (XRD) of: (A) octakis-hydridosilsesquioxane, $(HSiO_{3/2})_8$ and (B) octakis[3-(3-amino-1,2,4-triazole)propyl] octasilsesquioxane.

atoms of the $[Si_8O_{12}]$ framework, which agrees with a totally symmetrical and substituted structure.

The FTIR spectrum of the ATZ-SSQ is showed in Fig. 8. The spectrum clearly shows the symmetric stretchings of Si-O-Si peak at ~ 770 – 1100 cm^{-1} which corresponds to the silsesquioxane cage structure (1–7,20). The bands observed at 1320 , 1450 and 1620 cm^{-1} can be assigned to the $[\nu(C-N)]$, $[\nu(C-N)]$, and $[\delta(N-H)]$ deformation modes, respectively. The strong band at $\sim 1690\text{ cm}^{-1}$ can be assigned to the $[\nu(C=N)]$ ring deformation mode. The small peak at 2955 cm^{-1} can be attributed to the $[\nu(C-H)]$ deformation mode [2, 20]. The wide and strong band at $\sim 3500\text{ cm}^{-1}$ is assigned to the OH deformation due to H_2O . There is an absence of Si-H peak at $\sim 2250\text{ cm}^{-1}$, validating the structure containing [3-(3-amine-1,2,4-triazole)propyl]-substituted pendant groups on each vertex (2, 20).

All the above characterization methods provide the structure confirmation of ATZ-SSQ.

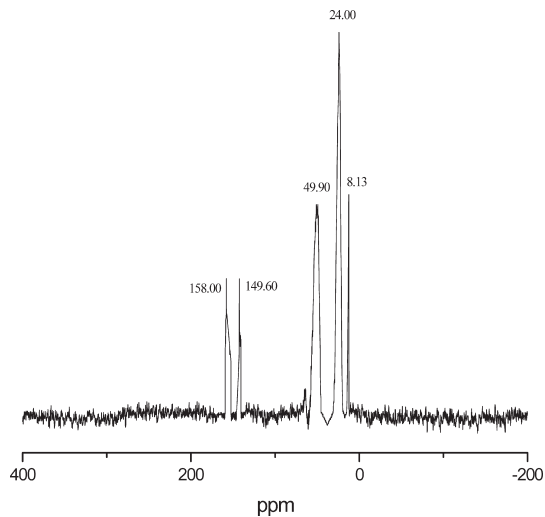


Figure 6. ^{13}C NMR spectrum of the octa[3-(3-amino-1,2,4-triazole)propyl]octa silsesquioxane.

Adsorption Isotherms

The effect of the time in the adsorption process was investigated, as is showed in Table 1. The equilibrium condition is reached very quickly for ATZ-SSQ,

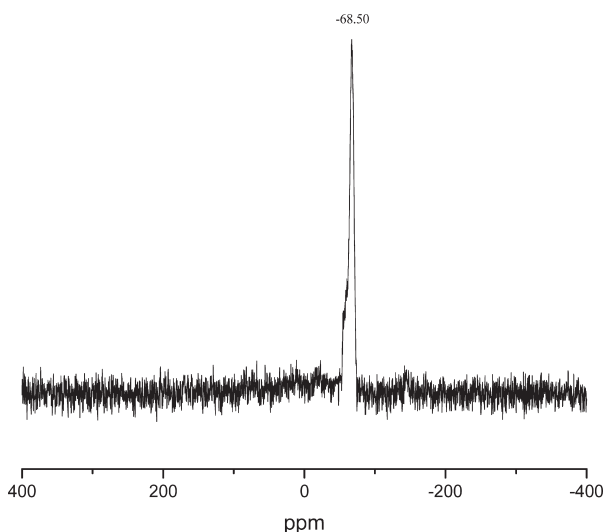


Figure 7. ^{29}Si NMR spectrum of the octa[3-(3-amino-1,2,4-triazole)propyl]octa silsesquioxane.

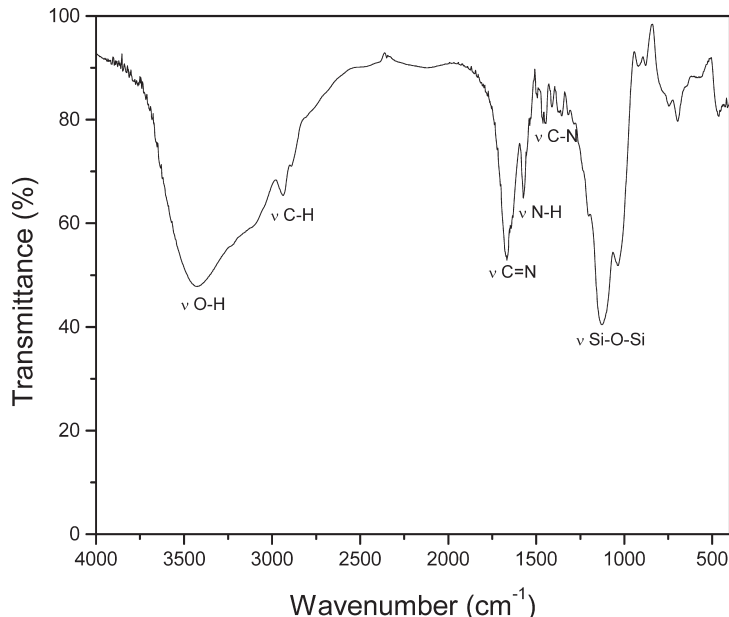


Figure 8. FTIR spectrum of the octakis[3-(3-amino-1,2,4-triazole)propyl]octa silsesquioxane.

indicating that the adsorption sites are well exposed on the surface of this kind of material. This interesting property of this nanomaterial permits to reach the maximal extraction quickly, at time lower than 3 min.

To verify the usefulness of the present nanomaterial for adsorption of Cu(II), Co(II), Fe(III), Zn(II), and Ni(II) from ethanol solutions, adsorption isotherms were determined.

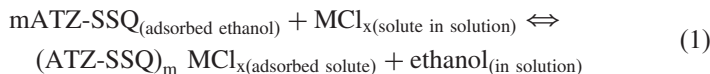
Table 1. The effect of time on the adsorption of transition-metal ions by ATZ-SSQ from ethanol solutions at 298K

Adsorbent	Time (min)	% Extraction of metal ions ^a				
		Cu(II)	Zn(II)	Fe(III)	Ni(II)	Co(II)
ATZ-SSQ	1	52.5	10.5	5.2	5.5	5.4
	3	90.6	17.9	10.5	9.0	9.3
	5	93.2	19.3	11.1	9.7	9.9
	10	93.1	19.5	11.9	9.6	9.0
	15	93.2	19.1	11.3	9.2	9.8
	25	93.0	19.3	11.1	9.5	9.3

^aBatchwise technique; 0.1 g of the adsorbent; 50.0 mL of 1.85×10^{-3} mol L⁻¹ ethanol solution of the metal ions

The organofunctionalized species on the solid surface behaves as a neutral ligand and, thus, MCl_x diffuses from the solution phase into the solid surface as a neutral species. These metal cations are coordinated to the nitrogen atoms of the 3-amino-1,2,4-triazole groups and the anions can be in the inner coordination sphere, bonded to the metal ion or remaining in the outer sphere, balancing the charge.

In any case, the metal adsorption process on the surface with the electrically neutral grafted ligands can be represented by the following complex formation equilibrium:



where M is Cu(II), Co(II), Fe(III), Zn(II), and Ni(II), and m is the number of ligands coordinating the transition-metal ions.

Plotting N_f against C , where C is the equilibrium concentration of the solute in solution phase, the adsorption isotherms for these five metals from ethanol solutions onto organofunctionalized surface are shown in Fig. 9. The same adsorption procedure with the octakis(3-chloropropyl) octasilsesquioxane showed that no cation was adsorbed.

Assuming that the adsorption process can be described by the Langmuir equation (28, 29):

$$C/N_f = C/N^s + 1/(K' - N^s) \quad (2)$$

the adsorption capacity, N^s , and the equilibrium constant, K' , were calculated

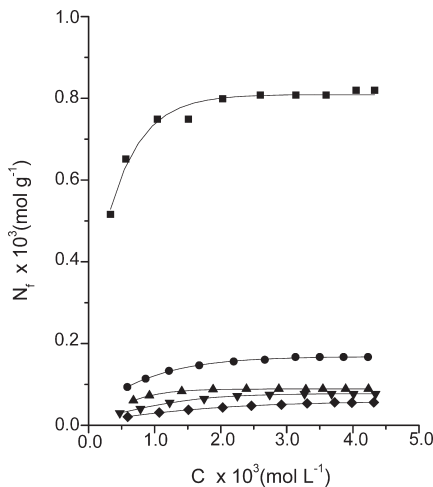


Figure 9. Adsorption isotherms of metal ions from ethanol solution on modified silsesquioxane at 298 K: (■) Cu(II); (●) Zn(II); (▲) Fe(III); (▼) Ni(II); (◆) Co(II).

by plotting C/N_f against C , according to Fig. 10. The calculated constants N^s and K' are presented in Table 2 together with the linear correlation coefficients r . The value of N^s is a constant which depends on the nature of the solvent, solute and temperature. The value of the maximal adsorption capacity, N^s , corresponds to the overall saturation of the available sites. The calculated values of maximal adsorption capacity, N^s , are in agreement with the experimental values, N_f . The surface complexes are thermodynamically stable, and the calculated constants for $(ATZ-SSQ)_m$ -transition metals complexes are very similar to those found for chemically modified silica surfaces (19, 20).

When dealing with the adsorption phenomena, the main assumption of the Langmuir model is that adsorption occurs uniformly on the active part of the surface and, when a molecule is adsorbed on a site, the latter does not have any effect upon other incident molecules. This seems to be in agreement with the results shown in Fig. 10.

The maximum metal ion uptake values for Cu(II), Co(II), Zn(II), Ni(II), and Fe(III) were 0.86, 0.10, 0.19, 0.09, and 0.09 mmol g^{-1} , respectively.

The ATZ-SSQ matrix can be used, without any significant loss of adsorption capacity, for various adsorption and desorption operations.

The degree of organofunctionalization exhibited by the ATZ-SSQ nanomaterial ($N_0 = 5.63 \text{ mmol g}^{-1}$) and, consequently, the adsorption capacity, is higher than that obtained by silsesquioxane 3-n-propylpyridiniumchloride polymer (SiPyCl) ($N_0 = 1.04 \text{ mmol g}^{-1}$) (8, 10), or silica surfaces chemically modified with organic molecules containing nitrogen atoms ($N_0 \cong 0.5 \text{ mmol g}^{-1}$) (16, 19, 20, 25), or organomodified barium phosphate ($N_0 \cong 1.3 \text{ mmol g}^{-1}$) (26). For instance, the adsorption capacities for the determination of

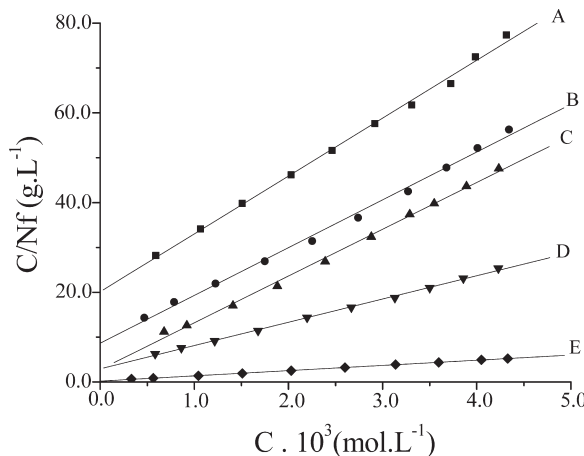


Figure 10. Adsorption isotherms of metal ions in ethanol solution on modified silsesquioxane as plot of C/N_f against C : (A) Co(II); (B) Ni(II); (C) Fe(III); (D) Zn(II); (E) Cu(II).

Table 2. Adsorption of metal ions by ATZ-SSQ from ethanol solutions at 298 K

Metal ion	N_f^a (mmol g ⁻¹)	N^S^b (mmol g ⁻¹)	K^b (L mol ⁻¹)	r
Cu(II)	0.84	0.86	5.8×10^3	0.999
Co(II)	0.09	0.10	3.8×10^3	0.998
Ni(II)	0.08	0.09	1.2×10^3	0.999
Fe(III)	0.09	0.09	0.6×10^3	0.998
Zn(II)	0.17	0.19	1.8×10^3	0.998

^a N_f = quantity of adsorbed metal.

^b N^S = adsorption capacity; K' = equilibrium constant.

Cu(II) from ethanol solution on SiPyCl (10) or organomodified silica surfaces (19, 20, 25) are 0.34 and ~ 0.25 mmol g⁻¹, respectively.

The adsorption process equilibrium condition is reached very quickly (3 min) for the ATZ-SSQ, probably due to high exposition of the adsorption sites. For instance, in the adsorption experiments in ethanol solution by batchwise technique was adopted a time of 3 h for shaken the organomodified barium phosphate with variable concentrations of each metal halide at a constant temperature of 298 K (26). This is an indication that the adsorption process equilibrium condition is only reached after a wide time interval.

Recovery and Determination of the Metal Ions

The results obtained (Table 3) from the experiments carried out in triplicate by passing each metal ion through the column packed with ATZ-SSQ showed that, in every case, the column retained the cations and they are then released by an acidic solution with nearly 100% efficiency. These values reflect a high efficiency for this organofunctionalized nanomaterial. The same procedure with the octakis(3-chloropropyl)octasilsesquioxane showed that no cation was adsorbed.

The recovery experiment for each metal ion from a synthetic solution served as basis for a rapid method for preconcentration and determination of metal ions in commercial ethanol, use as automotive engine fuel.

Table 4 shows the determination of the metal ions in samples of fuel ethanol produced in three different plants using columns packed with ATZ-SSQ. This high copper concentration in comparison with other metal ions can be explained by considering that this industrial operation uses a copper distillation column. The concentrations of Cu(II) in the analysed samples correspond to the contents of this metal normally found in fuel ethanol (16, 19, 20, 25, 26). The metal Co(II) was not found in detectable amount. In general, Co(II) does not occur in commercial ethanol (16). The content

of Fe(III) depends on the degree of corrosion of the distillation equipment. The concentration of Ni(II) normally found in the commercial ethanol is below $50 \mu\text{g L}^{-1}$ and Zn(II) is not detected when the conventional preconcentration method is used, in which the first step has been to evaporate the ethanol solution to dryness (16).

The data provided by plant 1, 2, and 3 indicated an amount of copper of 51, 60, and $78 \mu\text{g L}^{-1}$, and of iron of 20, 15, and $13 \mu\text{g L}^{-1}$, respectively, determined through atomic absorption. These values provided are very close to those determined in the experiments in our laboratory, using these same alcohols. Thus, these similar values demonstrated the accuracy of our laboratory determination. The results obtained are suitable for justifying the methodology used, which could be recommended for such cations found in commercial alcohol.

These retention capacities were not affected after several retention/elution cycles during 6 months of continuous use. The adsorbent material was resistant to the attack of concentrated acids, but not to the attack of concentrated aqueous alkali solution.

For cation determinations in fuel ethanol, the first step in the usual procedures has been evaporation of the liquid to dryness, which is obviously time-consuming (16). The proposed method improves the method of analysis extending the limit of detection to lower concentrations.

The advantage of the present method in comparison with other methods reported in the literature (16, 25, 26) is the high degree of organofunctionalization exhibited by the ATZ-SSQ nanomaterial ($N_0 = 5.63 \text{ mmol g}^{-1}$) and, consequently, the large adsorption capacity. These methods described in literature are based on organofunctionalized surfaces, such as organomodified silica and barium phosphate, which present degree of organofunctionalization (N_0) varying from 0.5 to 1.3 mmol g^{-1} .

An additional advantage of the nanomaterial based on silsesquioxane is that the adsorption process equilibrium condition is reached at time lower than 3 min, while for the organomodified barium phosphate nanomaterial (26) and for the organofunctionalized silica gel (16, 19, 20, 25) the equilibrium condition is only reached at times higher of 2.30 and 0.30 h, respectively.

Table 3. Recoveries of metal ions by ATZ-SSQ using the column method at 298 K, and 1.0 mol L^{-1} HCl solution as eluent ($n = 3$, 100 mL of $25 \mu\text{g L}^{-1}$ MCl_z ethanol solution, Volume of eluent = 5 mL)

Adsorbent	Ion	Recovery %
ATZ-SSQ	Co(II)	99.7 ± 0.5
	Cu(II)	99.8 ± 0.2
	Fe(III)	99.7 ± 0.3
	Ni(II)	99.8 ± 0.2
	Zn(II)	99.9 ± 0.2

Table 4. Determination of metal ions in commercial ethanol, used as fuel for car engines

Method	Plant	Concentration Found ($\mu\text{g L}^{-1}$)				
		Cu(II)	Zn(II)	Fe(III)	Ni(II)	Co(II)
ATZ-SSQ	1	51 \pm 1	7 \pm 1	20 \pm 1	9 \pm 1	^a
	2	60 \pm 2	8 \pm 1	15 \pm 1	10 \pm 1	^a
	3	78 \pm 2	9 \pm 1	13 \pm 1	14 \pm 1	^a

^aNot detected.

The ATZ-SSQ nanomaterial has great advantage for adsorption of these metal ions, due to its great stability, reutilization possibility, rapidity in reaching the equilibrium and high mechanical resistance.

CONCLUSIONS

The synthesis and characterization of the new nanomaterial based on organomodified silsesquioxane nanocages was reported. The characterization process confirms that eight 3-amino-1,2,4-triazole molecules were covalently linked to silsesquioxane nanoplatforms through of the eight pendant $(\text{CH}_2)_3\text{Cl}$ molecular “arms” of the octakis(3-chloropropyl)octasilsesquioxane, resulting in the formulation of octa[3-(3-amino-1,2,4-triazole)propyl]octasilsesquioxane (ATZ-SSQ).

The ATZ-SSQ matrix has been shown to be an effective solid-phase sorbent for copper, iron, zinc, nickel, and cobalt ions from ethanolic solutions. However, the ability of ATZ-SSQ to detect divalent metal complexes other than those used in this study is unknown.

The high degree of organofunctionalization associated with the large adsorption capacity, and the high chemical stability in ethanol suggest that the ATZ-SSQ may potentially be useful for analytical purposes in the determination of commercial ethanol, used as fuel for car engines.

The ATZ-SSQ nanomaterial has great advantage for adsorption of these metal ions, due to its great stability, reutilization possibility, rapidity in reaching the equilibrium and high mechanical resistance.

ACKNOWLEDGMENTS

N.L.D.F. is indebted to FAPESP and CNP₈ for the financial support.

REFERENCES

1. Waddon, A.J. and Coughlin, E.B. (2003) Crystal structure of polyhedral oligomeric silsesquioxane (POSS) Nano–materials: a study by x-ray diffraction and electron microscopy. *Chem. Mater.*, 15: 4555.
2. Phillips, S.H., Haddad, T.S., and Tomczak, S.J. (2004) Developments in nanoscience: polyhedral oligomeric silsesquioxane (POSS)-polymers. *Curr. Opin. Solid State Mater. Sci.*, 8 (1): 21.
3. Feher, F.J., Newman, D.A., and Walzer, J.F. (1989) Silsesquioxanes as models for silica surfaces. *J. Am. Chem. Soc.*, 111: 1741.
4. Provatas, A., Luft, M., Mu, J.C., White, A.L., Matisons, J.C., and Skelton, B.W. (1998) Silsesquioxanes: Part I: A key intermediate in the building of molecular composite materials. *J. Organomet. Chem.*, 565 (1–2): 159.
5. Baney, R.H., Itoh, M., Sakakibara, A., and Suzuki, T. (1995) Silsesquioxanes. *Chem. Rev.*, 95 (5): 1409.
6. Li, G.Z., Wang, V., Ni, H., and Pittman, C.U., Jr. (2001) Polyhedral oligomeric silsesquioxane (POSS) polymers and copolymer: A review. *J. Inorg. Organomet. Polym. Mat.*, 11: 123.
7. Calzaferri, G. (1996) *Tailor-Made Silicon-Oxygen Compounds*; Vieweg: Braunschweig.
8. Alfaya, R.V.S. and Gushikem, Y. (1999) Aluminum oxide coated cellulose fibers modified with *n*-propylpyridinium chloride silsesquioxane polymer: preparation, characterization, and adsorption of some metal halides from ethanol solution. *J. Colloid Interface Sci.*, 213 (2): 438.
9. Henden, B.J. and Marsmann, H.C. (1999) Silsesquioxanes as models of silica supported catalyst-I. [3-(diphenylphosphino)propyl]hepta[propyl]-[octasilsesquioxane] and [3-mercaptopropyl]-hepta[propyl]-[octasilsesquioxane] as ligands for transition-metal ions. *Appl. Organometal. Chem.*, 13 (4): 287.
10. Fujiwara, S.T., Gushikem, Y., and Alfaya, R.V.S. (2001) Adsorption of FeCl_3 , CuCl_2 and ZnCl_2 on silsesquioxane 3-*n*-propylpyridiniumchloride polymer film adsorbed on Al_2O_3 coated silica gel. *Colloids Surf.*, 178: 1–3.
11. Burleigh, M.C., Markowitz, M.A., Spector, M.S., and Gaber, B.P. (2002) Porous polysilsesquioxanes for the adsorption of phenols. *Environ. Sci. Technol.*, 36 (11): 2515.
12. Pozhidaev, Y.N., Panezhda, E.V., Grigor'eva, O.Y., Kirillov, A.I., Belousova, L.I., Vlasova, N.N., and Voronkov, M.G. (2003) Carbofunctional polyorganylsilsesquioxanes as sorbents for some rare metals. *Dokl. Chem.*, 389 (4–6): 97.
13. Dias Filho, N.L. and Gushikem, Y. (1997) 2-mercaptopimidazole covalently bonded to silica gel surface in selective separation of mercury(II) from an aqueous solution. *Sep. Sci. Technol.*, 32 (15): 2535.
14. Oshima, S.M., Perera, J.M., Northcott, K.A., Kokusen, H., Stevens, G.W., and Komatsu, Y. (2006) Adsorption behavior of cadmium(II) and lead(II) on mesoporous silicate MCM-41. *Sep. Sci. Technol.*, 41 (8): 1635.
15. Northcott, K., Kokusen, H., Komatsu, Y., and Stevens, G. (2006) Synthesis and surface modification of mesoporous silicate SBA-15 for the adsorption of metal ions. *Sep. Sci. Technol.*, 41 (9): 1829.
16. Moreira, J.C. and Gushikem, Y. (1985) Preconcentration of metal ions on silica gel modified with 3(1-imidazolyl)propyl groups. *Anal. Chim. Acta.*, 176: 263.
17. Dias Filho, N.L., Carmo, D.R., and Rosa, A.H. (2006) An electroanalytical application of 2-aminothiazole-modified silica gel after adsorption and separation of $\text{Hg}(\text{II})$ from heavy metals in aqueous solution. *Electrochim. Acta.*, 52: 965.

18. Jacques, R.A., Bernardi, R., Caovila, M., Lima, E.C., Pavan, F.A., Vaghetti, J.C.P., and Airoldi, C. (2007) Removal of Cu(II), Fe(III), and Cr(III) from Aqueous Solution by Aniline Grafted Silica Gel 42 (3): 591.
19. Dias Filho, N.L. (2006) Adsorption at surface-modified silica gels. In *Encyclopedia of Surface and Colloid Science*, 2nd Edn.; Taylor & Francis: New York, U.S.; Vol. 1, 229–241.
20. Dias Filho, N.L. and Carmo, D.R. (2006) Adsorption at silica, alumina, and related surfaces. In *Encyclopedia of Surface and Colloid Science*, 2nd Edn.; Taylor & Francis: New York, U.S., Vol. 1, p. 209–228.
21. Wang, S. and Zhang, R. (2007) Preconcentration and determination of copper in aqueous solution with epoxy resin-based monolithic column containing large interconnected pores. *Sep. Sci. Technol.*, 42 (5): 1079.
22. Guibal, E. and Vincent, T. (2006) Palladium recovery from dilute effluents using biopolymer-immobilized extractant. *Sep. Sci. Technol.*, 41 (11): 2533.
23. Modrzejewska, Z., Sujka, W., Dorabialksa, M., and Zarzycki, R. (2006) Adsorption of Cr(VI) on cross-linked chitosan beads. *Sep. Sci. Technol.*, 41 (1): 111.
24. Uheida, A., Iglesias, M., Fontàs, C., Zhang, Y., and Muhammed, M. (2006) Adsorption behavior of platinum group metals (Pd, Pt, Rh) on nonylthiourea-coated Fe_3O_4 nanoparticles. *Sep. Sci. Technol.*, 41 (5): 909.
25. Dias Filho, N.L., Gushikem, Y., Polito, W.L., Moreira, J.C., and Ehirim, E.O. (1995) Sorption and preconcentration of metal ions in ethanol solution with a silica gel surface chemically modified with benzimidazole. *Talanta*, 42: 1625.
26. Lazarin, A.M. and Airoldi, C. (2006) Layered crystalline barium phosphate organofunctionalized for cation removal. *Chem. Mater.*, 18: 2226.
27. Mantz, R.A., Jones, P.F., Chaffee, K.P., Lichtenhan, J.D., Gilman, J.W., Ismail, I.M. K., and Burmeister, M.J. (1996) Thermolysis of polyhedral oligomeric silsesquioxane (POSS) macromers and POSS-siloxane copolymers. *Chem. Mater.*, 8: 1250.
28. Adamson, A.W. (1990) *Physical Chemistry of Surfaces*, 5th Edn.; John Wiley & Sons: New York, U.S.
29. Langmuir, I. (1918) The adsorption of gases on plane surfaces of glass, mica and platinium. *J. Am. Chem. Soc.*, 40: 1361.